PAPER

Check for updates

Preparation of STF-loaded micron scale polyurethane polyurea double layer microcapsules and study on the mechanical properties of composites†

Wenyan Chen, Shuen Liang, Yan Peng, Yixia Wang and Tao Liu [ID] *

In this study, we report on a novel and effective approach for the encapsulation of the shear thickening fluid in polyurethane polyurea double layer microcapsules. Under the action of dibutyltin disilicate as a catalyst, CD-MDI reacted with polyethylene glycol to form polyurethane inner shell and reacted with diethylenetriamine to form a polyurea outer shell. The results show that the shear thickening liquid was emulsified using liquid paraffin as a solvent and Span80 as a surfactant to form a lotion similar to water-in-oil. The shear thickened droplets can be stably and uniformly dispersed to a diameter of 100 μm at a rotation speed of 800 rpm min^{-1}. The bilayer shell material achieves a good coating effect on STF, which provides support for strength and stress conduction and improves the compatibility between STF and polyurea matrix. The toughness and impact resistance of the composites were analyzed by a universal testing machine and drop hammer impact tester. Finally, compared with the pure polyurea material, the elongation at break of 2% added amount is increased by 22.70%, and the impact resistance of 1% added amount is the best, which is 76.81 N more than that of the pure specimen.

Introduction

With the increase in terrorism and international conflicts in the world, the development of high-performance protective materials has become a hotspot and challenge. In the early stage, rigid materials such as metals[1,2] and ceramics[3,4] are used to prepare high performance protective materials against mechanical impact. However, the disadvantages of being bulky, inflexible, and discomfort have limited their widespread use in the modern era. Therefore, materials with lightweight and good impact resistance are increasingly demanded to boost the safety factor in military (*e.g.*, body armor and protective coatings) and civilian settings (*e.g.*, sports protective equipment and labor protection).[5–7]

To obtain materials with lightweight and good impact resistance, shear thickening fluid (STF) is promoted, which is a non-Newtonian fluid as its shear viscosity increases significantly with the shear load, especially after a threshold shear rate.[8–10] Without any stimuli, the STF suspension system is fluid-like. When the external force is applied to the suspension system, the dispersed STF particles would change from the order state to the disorder state, and the clusters are formed,

which leads to a sharp increase in the viscosity.[11,12] However, once the external force is removed, the viscosity of the system quickly returns to the initial state.[13,14] Therefore, STF possesses the "solid–liquid" property, which endows it with excellent impact-resistant ability.[15,16] For example, the gel-Kevlar fabrics body armor material fabricated by STF and Kevlar has excellent impact resistance.[17,18] Under low-velocity drop tower loading, the maximum center force of the material is 5768 N, which is nearly half of neat Kevlar (11 414 N).[19]

To make the fluid-like STF practical, it is necessary to integrate it with a bulky material. However, the inert properties of STF, such as high viscosity, hygroscopicity, and fluidity as a liquid, make it difficult to handle or integrate into the structures. To date, strategies such as sandwich or closed-cell structure[20–22] are proposed to address the problem. However, the shear thickened property of the STF is hindered because of their rigid storage frames. Therefore, fabricating the STF composites without sacrificing the impact resistance ability has become a big problem.

It is well known to all that packaging STF by a polymer can enhance the interaction between STF and the matrix, which exerts the excellent rheological properties of STF. Besides, spherical cladding facilitates stress conduction and uniform distribution in the matrix, which broadens the scope of application of STF. For example, Liu *et al.* employed an orifice coagulation bath to produce capsules of STF.[23] STF capsules with an average diameter of 1.93 mm were successfully coated

Institute of Chemical Materials, China Academy of Engineering Physics, Mianyang 621900, Sichuan, China. E-mail: liutao_caep@163.com

† Electronic supplementary information (ESI) available: Analysis of thermal properties of composites, HN and VFT equations. See DOI: https://doi.org/10.1039/d2ra08111c

by studying the contents of calcium chloride solution, sodium alginate, and surfactant in different concentrations. Besides, Zhang and coworkers[24,25] reported an encapsulation method for STF. The solution composed of 85% STF, 5% PEI600, and 10% EDO was added dropwise through the needle tube into the reaction solution consisting of the diisocyanate prepolymer Suprasee 2644, toluene, and chloroform. The resulting capsules prepared by this method had an average diameter in the range of 0.2–2.7 mm. These strategies are effective to fabricate completely spherical STF capsules. However, due to the limited pore size of the needle tube, the size of the prepared capsule particles in these papers are too large, which makes the STF capsule difficult to disperse into matrix materials. In addition to that, these methods sacrifice the concentration of STF to be able to drop droplets from the needle, which results in a decrease in the shear thickening performance of the STF.

In this study, a method of encapsulating micron-scale STF microcapsules with polyurethane polyurea double shell is proposed. Firstly, under the emulsification of Span80, STF is well-dispersed in liquid paraffin to form droplets of about 100 μm. After that, the suspended droplets are successfully coated by a polyurethane/polyurea (PU/PUA) shell through interfacial polymerization. The microcapsule walls can provide excellent cladding effect and mechanical support, which can maximize the preservation of STF rheological properties and effectively improve the high speed impact resistance of polymer materials. In the end, the microcapsules can promote the mechanical properties of polyurea. Through the drop hammer test, the impact resistance of the polyurea composite is further improved by the addition of microcapsules.

Experimental

Materials

4,4′-Diphenylmethane diisocyanate modified by carbodiimide (CD-MDI) was purchased from Wanhua Chemical. Polyethylene glycol (PEG, with a molecular weight of 200 g mol^{-1}) was supplied by Chengdu Cologne. Silica microsphere (SiO$_2$, 10% w/v ethanol suspension) was provided by Weng Jiang Reagent. Liquid paraffin was provided by Aladdin. Diethylenetriamine (DETA) was provided by Aladdin. Dibutyltin disilicate (DBTL) was provided by Aladdin. Span80 was provided by Aladdin. Toluene was purchased from Sinopharm. Polytetramethylene ether diol di-p-aminobenzoate (P1000) was provided by Shenglong Chemical. All reagents in this study were used without any further purification unless otherwise specified.

Preparation of polyurea polyurethane bilayer STF microcapsules

31 g nanosilica, 19 g polyethylene glycol, and 50 g absolute ethanol were mixed and stirred for 10 min by a planetary stirrer. After drying in a vacuum oven to remove absolute ethanol and deformation by ultrasonication for 30 min, STF was obtained. Then, 1.00 g STF, 18.75 g liquid paraffin, and 0.10 g Span80 were mixed and stirred for 10 min with a magnetic bar at 800 rpm to obtain an emulsion. After adding 10 μL dibutyltin disilicate and

0.1 mL carbodiimide-modified 4,4′-diphenylmethane diisocyanate, the emulsion was stirred for 10 min. After the above steps, 0.05 mL diethylenetriamine was added to the reaction solution, and the mixture was stirred for 5 min. After this, the mixture was washed with toluene three times, followed by drying in a vacuum oven at 60 °C for 8 h to obtain polyurea polyurethane bilayer STF microcapsules.

Preparation of composite materials

16.00 g P1000, 4.00 g CD-MDI, and 1.05 g polyurethane polyurea bilayer STF microcapsules were mixed and stirred for 2 min by a planetary stirrer. It was poured into a Teflon mold and cured at room temperature for 24 h, followed by curing in an oven at 60 °C for 24 h to give a 1 mm thick composite polyurea material (PM-STF-PUA). The preparation method of pure polyurea sample was consistent with the above method but the microcapsule addition amount was 0%.

Characterization

A strain-controlled rheometer (ARES G2) was used to measure the shear-strain-dependent rheology of the STF. Dynamic frequency sweeps was carried out using 20 mm diameter parallel plates with a gap of 1 mm at shear rates ranging from 0 to 150 s^{-1}.

The droplet morphology of the STF emulsion was observed by a KH-8700 optical microscope.

The morphologies of the cross-sections of the microcapsules and composites were observed by scanning electron microscopy (SEM), and the samples were vacuum gold-sprayed before testing.

The chemical structures of the microcapsules and raw materials were conducted by Fourier transform infrared spectroscopy (FT-IR) using a Bruker TENSOR 27 attenuated total reflectance (ATR) system. The samples were scanned averaging 32 scans over the wave number range from 4000 cm^{-1} to 400 cm^{-1} with a resolution of 4 cm^{-1}.

Thermogravimetric analyzer (TGA, Q500) was used to analyze the thermal stability and core content of the prepared microcapsules by comparing the TGA traces of the microcapsules, core, and shell materials sing a sample weight of 8 mg with a heating rate of 10 °C min^{-1} over the temperature range of 25–800 °C under a nitrogen atmosphere.

Dynamic mechanical tests of PM-STF-PUA were performed by the dynamic mechanical analysis machine (RSA G2) with shear pattern. Samples were cut into small dumbbell with 10 mm length, 2 mm width, and 1 mm thickness. The measurements were conducted at 1 Hz at heating rates of 3 °C min^{-1} from −80 to 120 °C.

The tensile strength and elongation at break of the composites were tested by the universal testing machine WDW-50F with a tensile rate of 200 mm min^{-1}. Specimens were trimmed into a dumbbell type with a test length of 10 mm, which was wrapped with abrasive paper and adhesive cloth on both ends to prevent slippage. For each formulation, at least five replicate samples were tested for statistical accuracy.

The impact resistance of the composites was studied on a drop hammer. A steel conical tip with a mass of 32 g was used as an impactor. The single layer 35×35 mm^2 specimen was securely clamped between two steel plates. The impactor dropped freely from the height of 50 cm. The acceleration sensor was set on the base to record the force changes during the impact.

Dielectric measurements of the samples were recorded using a Novocontrol broadband dielectric relaxation spectroscopy (BDRS) in the frequency range of 10^{-2} to 10^7 Hz with a diameter of 20 mm and a thickness of about 1 mm. The dielectric cell was electrically shielded in nitrogen gas atmosphere and isothermal frequency scans were conducted in the temperature range of -120 to 150 °C in steps of 5 °C. Temperature was controlled by a Quattro system within $\pm$ 0.1 °C. Experimental data were theoretically analyzed using WinFit software supplied by Novocontrol.

Preparation of microcapsules

As shown in Fig. 1, the preparation of the dual shell microcapsules includes three steps. Firstly, a micron-sized emulsion was firstly obtained after stirring the mixture of STF, liquid paraffin, and Span80 (as emulsifier) at a low rotation speed (Fig. 1(a)). Then, the polycondensation occurs between the PEG in the STF droplets and CD-MDI at the surface of the emulsion to form a preliminary polyurethane shell layer (Fig. 1(b)). Finally, the unreacted isocyanate on the surface of polyurethane shell layer reacts with DETA to form a dense polyurea shell layer (Fig. 1(c)). As a result, dual shell microcapsules are formed.

The dispersed particles adopted for the preparation of STF are solid silica microspheres with a particle size of about 150 nm, which plays a decisive role in the shear thickening performance of STF, as shown in Fig. 1(e). To investigate the shear thickening property of the STF, the rheological tests of STF with different silica concentrations are carried out (details in ESI†). As shown in Fig. 1(f), the viscosity of SiO$_2$/PEG200 fluids firstly decreases with the increase in the shear rate, then increases rapidly after a critical shear rate is reached. The higher the concentration of silica, the lower the critical shear rate and the faster the viscosity mutation. When the concentration of silica is 68.5%, after a critical shear rate at 60 s^{-1} was reached, the viscosity increases rapidly and the value at the peak was 28 times larger than the initial value. To make sure that STF can be suspended in the solvent, the STF with lower concentration (62.0%) is chosen. Nevertheless, the consumption of PEG during the following reaction process will increase the concentration of silica, which ensures the good shear thickening performance (details in ESI†). This ingenious design not only ensures the dispersion of STF but also maintains good shear thickening performance.

The emulsification effect of STF in liquid paraffin was observed by optical microscopy and the prepared double-layered microcapsules, and the cross-sections of composites were observed by SEM, as shown in Fig. 2(a). It can be seen from Fig. 2(a1) and (a4) that STF emulsification in liquid paraffin is well dispersed. The average droplet diameter is 100 μm with an agitation rate of 800 rpm. As shown in Fig. 2(a2) and (a3), the spherical particle size and double layered microcapsule wall are 190 μm and 14.31 μm, respectively. The surface of the microcapsules has a certain roughness, which is believed to be caused by the uneven shrinkage of wall materials caused by the rapid evaporation of solvent in the drying process and the certain
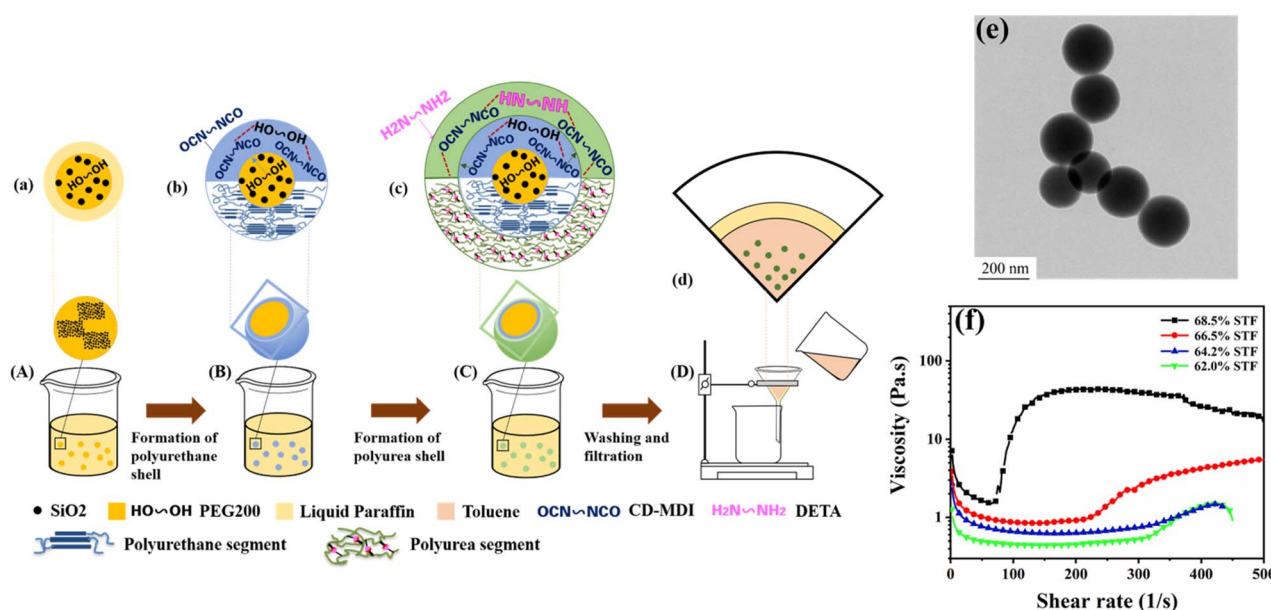

Fig. 1 Schematic illustration of the preparation of STF microcapsules with a PU/PUA double-walled shell by interfacial polymerization. (a) STF droplets dispersed in liquid paraffin; (b) STF microcapsules coated with polyurethane monolayer; (c) STF microcapsules coated with polyurethane polyurea double layer; (d) washing and filtration process; (e) TEM image of silica microspheres contained in STF; (f) variation of shear thickening with shear rate in different silica concentrations of STF.
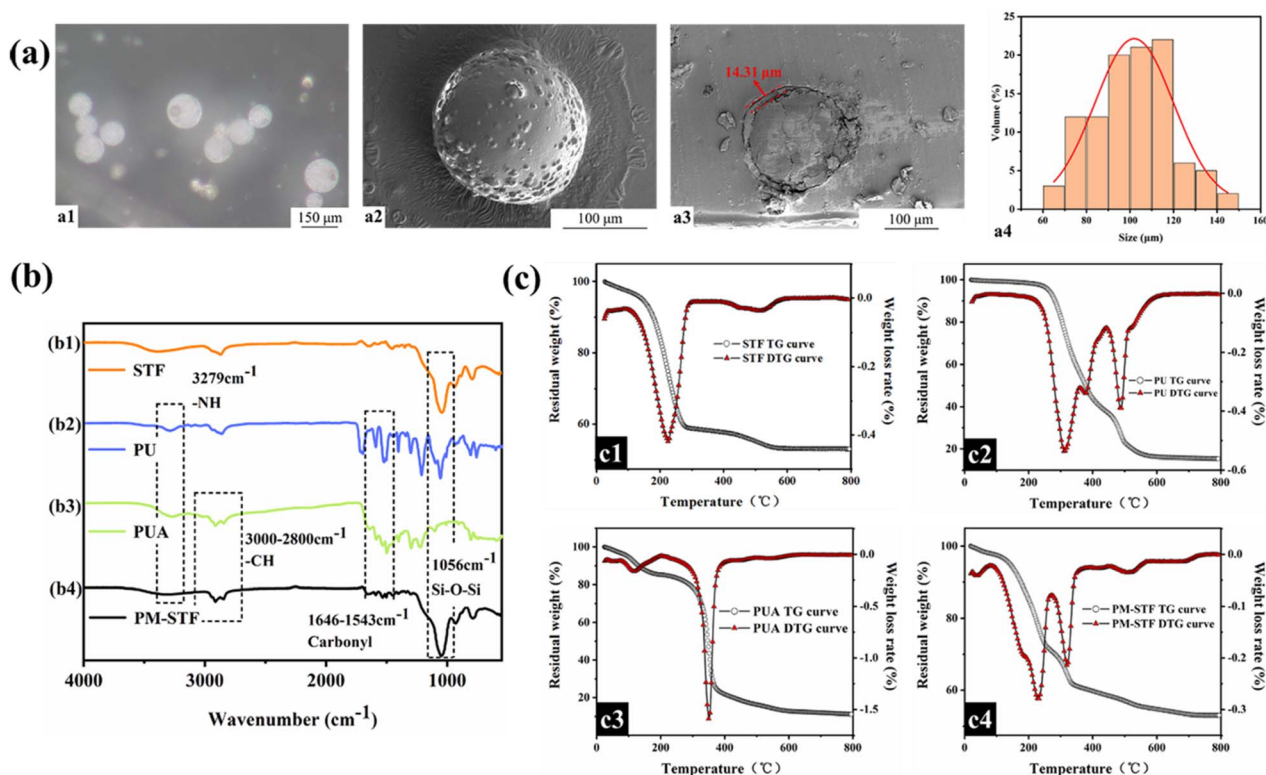
Fig. 2 (a) Microcapsule topography of (a1) emulsion under an optical microscope; (a2) microcapsules under an electron microscope; (a3) cross-section of composite material under an electron microscope; (a4) size distribution of microcapsules. (b) Infrared spectra of (b1) STF; (b2) PU shell; (b3) PUA shell; and (b4) microcapsules. (c) TGA curves of (c1) core materials; shell materials (c2) PU and (c3) PUA; (c4) microcapsules.

adhesion between microcapsules in the emulsion reaction. We also used drop addition to prepare STF capsules for comparison (details in ESI†).

To investigate the structure of the core material, pure wall material, and microcapsules, the FTIR test was carried out, and the results are shown in Fig. 2(b). The peak at 1082 cm^{-1} corresponds to the asymmetric and symmetric vibrations of the Si–O–Si groups of the silica microspheres in the core material STF, which could also be observed in the spectra of the microcapsules. In the spectra of b2 and b3, the carbonyl peaks in the range of 1646–1543 cm^{-1} and the peak of the stretching vibration of –NH at 3279 cm^{-1} are observed. The same absorption peak also appears in the spectra of microcapsules, which confirms the formation of polyurea and polyurethane. By comparing the spectra of b3 and b4, the microcapsules and polyurea have the same characteristic absorption peaks at 2922 cm^{-1} and 2854 cm^{-1}, which further indicates that the outermost layer of the microcapsules is the polyurea shell. According to the infrared spectrum, the absorption characteristic peaks of the STF and the polyurea-polyurethane shell can be observed, which confirms the successful encapsulation of STF within the microcapsules.

Besides, the thermogravimetric analysis of the double-layered microcapsules, pure core material, and pure wall material are shown in Fig. 2(c). According to Fig. 2(c1), the STF shows only one thermal degradation stage from 150 °C to 370 °C, which corresponds to the thermal decomposition process of

the PEG contained in it. The weight of the pure core material (STF) decreases rapidly at 225 °C. In comparison, the microcapsule with STF as the core shows two weight loss stages (Fig. 2(c4)), indicating the successful encapsulation of STF in the PU/PUA shell. Moreover, the initial decomposition temperature of the microcapsule is quite close to that of the STF, which indicates that the weight loss of the first stage at 240 °C mainly arises from the volatilization and decomposition of the STF. By comparing Fig. 2(c2–c4), it clearly shows that the decomposition temperature of the polyurethane shell and polyurea shell is 320 °C, proving that the core material has a good coating effect under PU and PUA shell. Compared to Fig. 2(c1), the thermal weight loss temperature point of STF in microcapsule increases from 225 °C to 240 °C and the weight loss speed of STF slows down. This indicates that the polyurea polyurethane double-layered microcapsules have good thermal protection to the core material. The polyurea polyurethane shell can not only improve the service temperature of STF but also slows down the leakage of STF.

The mechanical properties of composite materials

Because polyurea itself has good impact resistance and mechanical properties, it is not easy to improve its performance by adding fillers. However, the addition of this microcapsule can increase the storage modulus of the composite material (details in ESI†) and further improve its impact resistance. As shown in Fig. 3(a), polyurea materials with different microcapsule
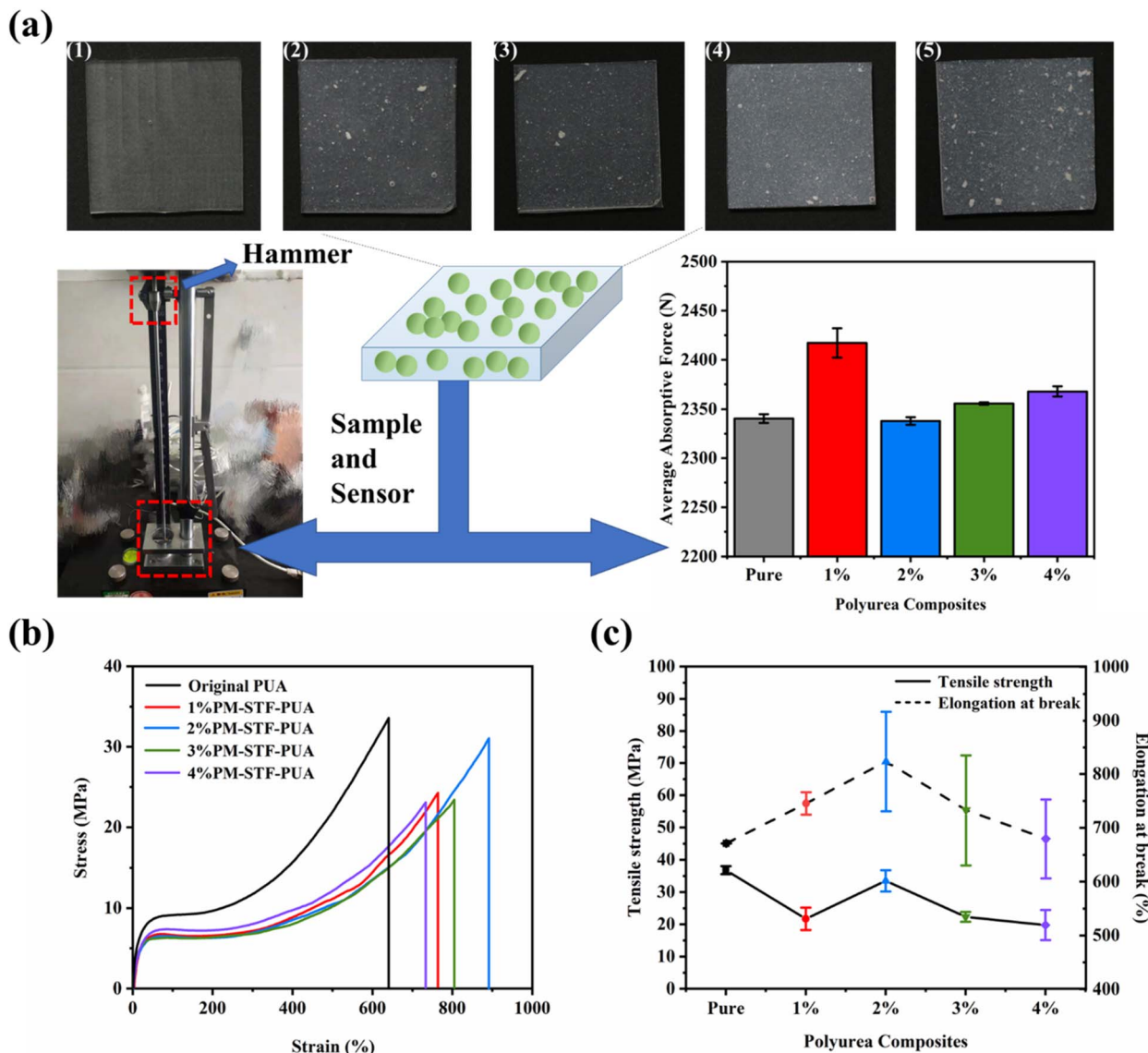
Fig. 3 Mechanical properties of composite materials with different microcapsule content (1: pure; 2: 1%; 3: 2%; 4: 3%; 5: 4%) (a) schematic diagram of drop hammer impact test and impact resistance of composites; (b) stress−strain curve of composite during the tensile process; (c) tensile strength and elongation at break of the composites.

additions are cut into squares with the size of 35 × 35 mm. With the addition of microcapsules increasing from 1% to 4%, the average impact force obtained from the sensor firstly increases and then decreases, which reflects that the impact resistance of PUA specimens firstly decreases and then increases. This trend can be illustrated by the negative correlation between synergistic segment motion ability and shock resistance of the soft segment of polyurea (Table 1). Both the innate properties of microcapsules and the its dispersion in the matrix will affect the properties of the composites. Firstly, microcapsules have good impact resistance, which can improve the impact resistance effect of composite materials. Moreover, soft microcapsules are beneficial to improve the movement of chain segments in composite materials, while an excess amount of microcapsules will form aggregates, as shown in Fig. 3(a), thus affecting the movement of

segments. Compared with the pure PUA specimens, the impact resistance of 1% added amount is the best, which is 76.81 N more than that of the pure specimen.

To investigate the mechanical property, the uniaxial tension experiment is carried out and the results are shown in Fig. 3(b)

Table 1 The Vogel−Fulcher−Tamman (VFT) fitting parameter, B, $\ln(f_0/\text{Hz})$, and the T_0 values obtained by broadband dielectric spectroscopy

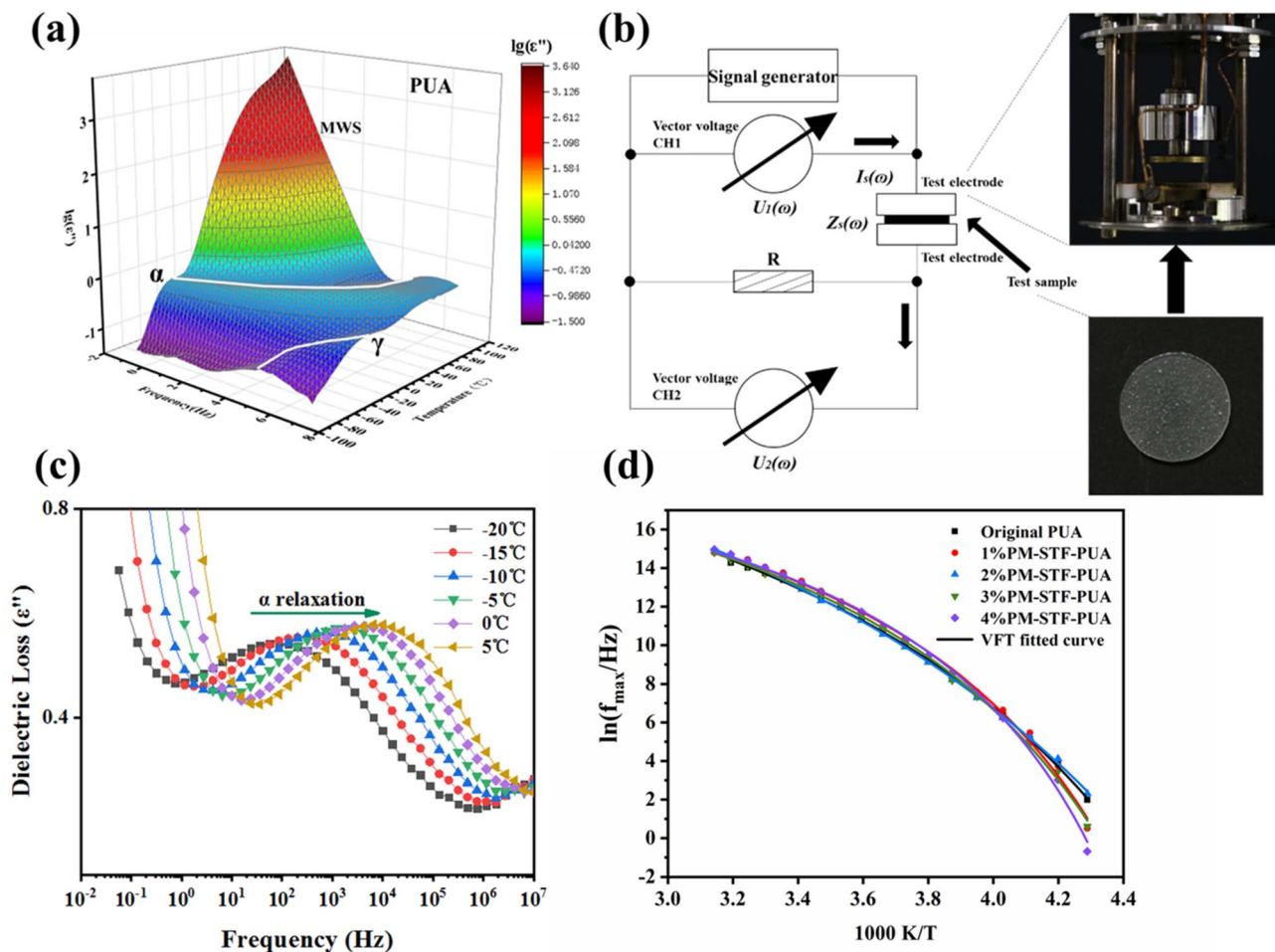| Sample	$\ln(f_0/\text{Hz})$	B (K)	T_0 (K)
Original PUA	24	1347	172
1% PM-STF-PUA	22	863	191
2% PM-STF-PUA	26	1839	156
3% PM-STF-PUA	22	963	188
4% PM-STF-PUA	21	727	199

Fig. 4 (a) Three-dimensional plot of the dielectric loss *vs.* temperature and logarithm of the frequency for the PUA sample; (b) dielectric broadband energy spectrum test; (c) curve of dielectric loss with frequency of polyurea composites with 1% PM-STF addition under different temperature conditions. (d) The relationship curve of the maximum relaxation frequency of the polyurea α relaxation process and the temperature (1000/T) under different additions, together with the corresponding fits to the VFT law.

and (c). The tensile strength of the PUA samples with different content of microcapsules decreases slightly compared to the pure PUA because the microcapsule packing affects the microphase structure of the polyurea. This can be attributed to the dominant role of the matrix polyurea on the mechanical properties of the composites. The presence of fillers reduced the content and continuity of the polyurea, thus degrading the mechanical properties of the composites. Soft microcapsules are beneficial to improve the movement of the chain segments in the composite and increase the elongation at break of the composite, while excessive microcapsules will form aggregates, which will affect the movement of the chain segments. The 2% added sample shows the best tensile strength and fracture elongation. With the increase in microcapsule additions, both the tensile strength and elongation at break of the composites firstly increase and then decrease.

Molecular mobility of composite materials

To figure out the reason why the microcapsule can increase the mechanical and impact properties, the molecular dynamics in

the polyurea elastomers were investigated by means of broadband dielectric spectroscopy over a wide temperature range (Fig. 4(b)).[26] Frequency and temperature dependencies of the dielectric losses for the pure polyurea elastomer are shown in Fig. 4. As shown in Fig. 4(a), the 3D diagram of pure PUA shows two relaxation mode, α and γ, which is corresponding to the segment motion in the hard and soft phase, respectively. Meanwhile, electrons or ions accumulate at the interface of the soft and hard phases, leading to a very strong Maxwell–Wagner–Sillars (MWS) interface polarization peak.

Fig. 4(c) is the dielectric loss of composite (1%PM-STF addition) *versus* frequency at different temperatures. All curves have a strong relaxation peak at intermediate frequencies, which moves rapidly to a high frequency with the increase in temperature. This relaxation corresponds to concerted segment motion of the soft segments, which illustrates that the cooperative segment motion of the soft segment gradually strengthens with the increase in temperature, and the α relaxation process is strongly temperature-dependent.

By fitting the curve in Fig. 4(c) with HN and VFT equations (details in ESI†), the B, ln(f_0/Hz), and the T_0 values are obtained

(Table 1). As shown in Table 1, it is worth noting that T_0 firstly decreases and then increases as the amount of microcapsules increases from 1% to 4%. This illustrates that the amount and distribution of microcapsules jointly influence the synergistic segment motion ability of soft segments. Soft microcapsules are beneficial to improve the movement of the chain segments in the composite, and T_0 gradually decreases with the increase in the microcapsule content at low content. On the other hand, large amount of microcapsules will form aggregates, as shown in Fig. 3(a), thus affecting the movement of segments, and T_0 will gradually increase. This result is consistent with the variation trend of the mechanical properties measured previously by a universal testing machine.

Conclusion

In summary, micron scale STF microcapsules possessing good shear thickening effect are successfully synthesized using an interface aggregation process by dispersing STF droplets into a reaction solution. Liquid paraffin plays a key role as a solvent during the emulsification process because it can regulate the density and polarity of the reaction solution so that STF is well dispersed and suspended in it. Polyurethane and polyurea bilayer shells can form a good coating effect on STF. The polyurethane shell layer plays a preliminary stereotypic role in the STF droplets, while the polyurea shell layer provides more solid protection. The polymer microspheres in this study formed a good adhesive interface with the polyurea. With the increase in microcapsule additions, both the impact resistance and elongation at break of the composites improve, and the tensile strength of the composites decreases. STF-loaded microcapsules improve the impact resistance of composite materials. The dielectric spectrum VFT equation fitting parameters of the composites is consistent well with the variation trend of the mechanical properties measured previously by the universal testing machine. Soft microcapsules are beneficial to improve the movement of the chain segments in the composite at low content, while a large amount of microcapsules will form aggregates, thus affecting the movement of segments. The encapsulation technique for producing STF microcapsules with high impact resistance and ability to absorb strain energy provides a new approach for designing and fabricating multifunctional impact-resistant materials.

Author contributions

Wenyan Chen: writing – original draft (lead). Shuen Liang: supervision (equal). Yan Peng: supervision (equal). Yixia Wang: validation (equal). Tao Liu: project administration (lead).

Conflicts of interest

There are no conflicts to declare.

Acknowledgements

References

1 G. M. Zhang, R. C. Batra and J. Zheng, *Composites, Part B*, 2008, **39**, 476–489.
2 M. B. Karamis, A. A. Cerit and F. Nair, *J. Compos. Mater.*, 2008, **42**, 2483–2498.
3 S. Feli and M. R. Asgari, *Composites, Part B*, 2011, **42**, 771–780.
4 P. Tan, *Mater. Des.*, 2014, **64**, 25–34.
5 S. Wang, S. Xuan, W. Jiang, W. Jiang, L. Yan, Y. Mao, M. Liu and X. Gong, *J. Mater. Chem. A*, 2015, **3**, 19790–19799.
6 S. E. Atanasov, C. J. Oldham, K. A. Slusarski, J. Taggart-Scarff, S. A. Sherman, K. J. Senecal, S. F. Filocamo, Q. P. McAllister, E. D. Wetzel and G. N. Parsons, *J. Mater. Chem. A*, 2014, **2**, 17371–17379.
7 X. G. Chen, Y. Zhou and G. Wells, *Composites, Part B*, 2014, **58**, 35–42.
8 E. Brown, N. A. Forman, C. S. Orellana, H. Zhang, B. W. Maynor, D. E. Betts, J. M. DeSimone and H. M. Jaeger, *Nat. Mater.*, 2010, **9**, 220–224.
9 N. J. Wagner and J. F. Brady, *Phys. Today*, 2009, **62**, 27–32.
10 W. J. Wen, X. X. Huang, S. H. Yang, K. Q. Lu and P. Sheng, *Nat. Mater.*, 2003, **2**, 727–730.
11 A. Majumdar, B. S. Butola and A. Srivastava, *Mater. Des.*, 2014, **54**, 295–300.
12 A. Haris, H. P. Lee, T. E. Tay and V. B. C. Tan, *Int. J. Impact Eng.*, 2015, **80**, 143–151.
13 E. Brown and H. M. Jaeger, *Rep. Prog. Phys.*, 2014, **77**, 046602.
14 R. Mari, R. Seto, J. F. Morris and M. M. Denn, *J. Rheol.*, 2014, **58**, 1693–1724.
15 N. Fernandez, R. Mani, D. Rinaldi, D. Kadau, M. Mosquet, H. Lombois-Burger, J. Cayer-Barrioz, H. J. Herrmann, N. D. Spencer and L. Isa, *Phys. Rev. Lett.*, 2013, **111**, 108301.
16 W. F. Jiang, X. L. Gong, S. H. Xuan, W. Q. Jiang, F. Ye, X. F. Li and T. X. Liu, *Appl. Phys. Lett.*, 2013, **102**, 101901.
17 Q. He, S. Cao, Y. Wang, S. Xuan, P. Wang and X. Gong, *Composites, Part A*, 2018, **106**, 82–90.
18 T. J. Kang, C. Y. Kim and K. H. Hong, *J. Appl. Polym. Sci.*, 2012, **124**, 1534–1541.
19 C. Zhao, Y. Wang, S. Cao, S. Xuan, W. Jiang and X. Gong, *Compos. Sci. Technol.*, 2019, **182**, 107782.
20 X. Wu, K. Xiao, Q. Yin, F. Zhong and C. Huang, *Int. J. Mech. Sci.*, 2018, **138**, 467–475.
21 C. Caglayan, I. Osken, A. Ataalp, H. S. Turkmen and H. Cebeci, *Compos. Struct.*, 2020, **243**, 112171.
22 M. Soutrenon and V. Michaud, *Smart Mater. Struct.*, 2014, **23**, 035022.
23 X. Liu, J.-L. Huo, T.-T. Li, H.-K. Peng, J.-H. Lin and C.-W. Lou, *Polymers*, 2019, **11**(3), 519.
24 H. Zhang, X. Zhang, Q. Chen, X. Li, P. Wang, E.-H. Yang, F. Duan, X. Gong, Z. Zhang and J. Yang, *J. Mater. Chem. A*, 2017, **5**, 22472–22479.
25 X. Zhang, H. Zhang, P. F. Wang, Q. Chen, X. Li, Y. J. Zhou, X. L. Gong, Z. Zhang, E. H. Yang and J. L. Yang, *Compos. Sci. Technol.*, 2019, **170**, 165–173.
26 N. Sebastian, C. Contal, A. Sanchez-Ferrer and M. Pieruccini, *Soft Matter*, 2018, **14**, 7839–7849.